



Moho depth variation in Taiwan from teleseismic receiver functions

Hsiao-Lan Wang^a, Lupei Zhu^{b,*}, How-Wei Chen^c

^a Institute of Seismology, National Chung Cheng University, Chia-Yi 621, Taiwan

^b Department of Earth and Atmospheric Sciences, Saint Louis University, MO 63108, USA

^c Institute of Geophysics, National Central University, Chung-Li 32001, Taiwan

ARTICLE INFO

Article history:

Received 6 March 2009

Received in revised form 20 August 2009

Accepted 27 August 2009

Keywords:

Receiver function

H - κ stacking

Crustal thickness

Taiwan

ABSTRACT

We determine lateral variation of Moho discontinuity, crustal thickness, and V_p/V_s ratios in the vicinity of Taiwan by analyzing all the available teleseismic waveform data collected by the Broadband Array in Taiwan for Seismology network from 1998 to 2004. The crustal thickness and the average crustal V_p/V_s ratio beneath each station are obtained by stacking Ps, PpPs and PpSs + PsPs phases coherently. The best estimated crustal thickness of Taiwan from 27 broadband stations is 30 km on average. The thinnest crust (11–15 km) is found east of the Longitude Valley suture zone, as part of the oceanic crust of the Philippine Sea plate. In other places, the crustal thickness varies from 17–19 km in northern Taiwan to 32–39 km in the southwestern island. The deepest Moho is found to be 53 km beneath station SSLB in central Taiwan. The average crustal V_p/V_s ratio in Taiwan is 1.74, with higher values of 1.74–1.99 in the north and lower values of 1.60–1.74 in the south. The crustal thickness variation is supported by gravity measurements in Taiwan and indicates that the collision between the Philippine Sea plate and Eurasian plate in Taiwan involves the whole crust. The thin crust and high V_p/V_s ratios in northern Taiwan are believed to be related to the volcanism in Tatun and Keelung located in the southwestern extent of the Okinawa Trough.

© 2009 Elsevier Ltd. All rights reserved.

1. Introduction

Taiwan is located at the junction of the Ryukyu subduction system in the north and the Manila subduction system in the south (Fig. 1). It is believed that the active orogeny in Taiwan was generated by the collision between the Eurasian continental plate and Philippine Sea plate since Cenozoic (Lin and Watts, 2002). There are several models proposed to explain the tectonic development of Taiwan (e.g. Suppe, 1981; Hsu and Sibuet, 1995; Wu et al., 1997; Teng and Lin, 2004; Lin et al., 2003; Sibuet and Hsu, 2004), including the thin-skinned tectonics (Suppe, 1981) and the lithospheric collision model (Wu et al., 1997). In the past two decades, seismic tomographic studies provided the overall crustal structure of Taiwan (e.g. Roecker et al., 1987; Shin and Chen, 1988; Rau and Wu, 1995; Ma et al., 1996; Kim et al., 2005). The most recent tomographic study by Wu et al. (2007, 2009) confirmed crustal V_p structure in previous studies and provided better constraint on crustal V_p/V_s ratios. In their results, the Luzon volcanic arc is characterized as a belt of high V_p and high V_p/V_s at depths between 13 and 25 km. This high V_p/V_s belt can be traced to the subduction zone between Hualien and Ilan (from station HWAB–NANB in Fig. 1) in the deeper portion. The shallow portions of the south-

western coastal plain and the Pingtung region (from station WSSB to SCZB) are also characterized by a belt of high V_p/V_s , which may be caused by water-saturated young sediments. The study also suggests that there is a low V_p/V_s belt and a mountain root beneath the Central Ranges. However, due to sparse data, the crustal structure of the aseismic zones in the western foothill and central Taiwan is still poorly defined.

To derive velocity structure of deep crust and uppermost mantle for Taiwan, an alternative method called receiver function analysis is used in this study. The receiver function method provides high resolution information down to at least lithospheric depths by using teleseismic waveform data (Ammon, 1991; Langston, 1979). The interface between crust and mantle is often called the “Moho discontinuity”, which exhibits a large acoustic impedance difference in seismic properties. Based on theoretical study (e.g. Phinney, 1964; Zhu et al., 1993), the P-to-S converted wave (Ps) generated at the Moho discontinuity will show dominantly on the radial receiver functions. We can utilize this Ps phase arrival time and amplitude to study the crustal structure and lateral variation of the Moho depth beneath Taiwan.

The first receiver function study in the Taiwan region was carried out by Tomfohrde and Nowack (2000) using frequency-band inversion of six short-period stations of the Taiwan Seismic Network (TSN). They provided a simple 1D crustal model beneath each station. The average Moho depth from all six stations is 38 km below sea level. Kim et al. (2004) showed that the average Moho

* Corresponding author.

E-mail addresses: hsiaolan.wang@gmail.com (H.-L. Wang), lupei@eas.slu.edu (L. Zhu), hwchen@earth.ncu.edu.tw (H.-W. Chen).

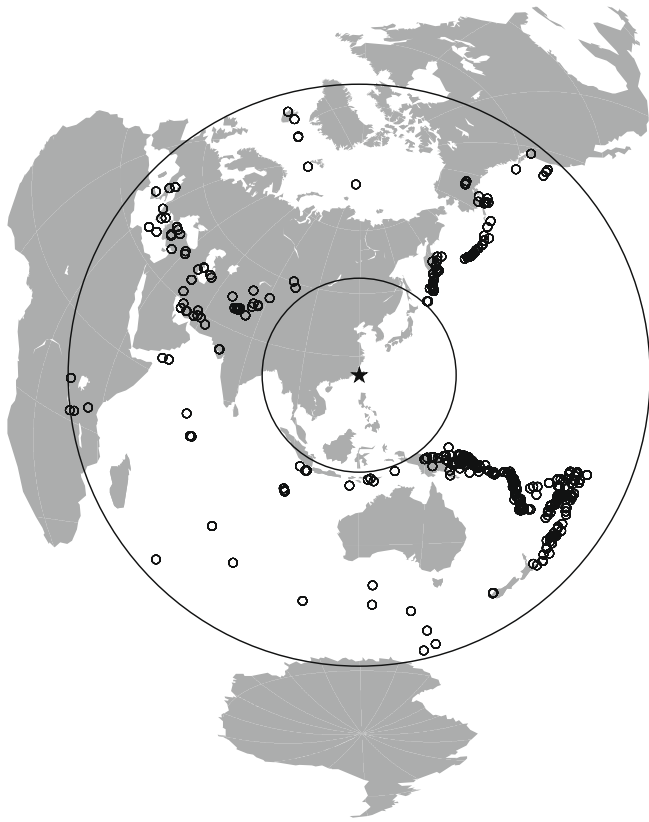


Fig. 2. Map showing epicenters of the selected teleseismic events (open circles) used in this study. The two large circles represent epicentral distances of 30° and 90°. The center of map (bold star) is (120.0°E, 24.0°N).

3. Methodology

The crustal thickness at each station was estimated from the Moho P-to-S converted phase and its later crustal multiples shown on the radial receiver functions. In order to remove the source and

instrument effects, receiver functions were obtained by using a time-domain iterative deconvolution technique (Ligorria and Ammon, 1999). We used a Gaussian low-pass filter to suppress noise above 1 Hz in the receiver functions. Then the receiver functions were rotated to the radial and tangential directions. Receiver functions from clustered events were stacked to increase the signal-to-noise ratio. We used the H - κ stacking method of Zhu and Kanamori (2000) to estimate crustal thickness and Vp/Vs ratio for each station. The technique sums the amplitudes of Moho Ps and its crustal multiples (PpPs and PpSs + PsPs) using different crustal thicknesses (H) and Vp/Vs ratios (κ). The best crustal thickness and Vp/Vs ratio are determined by the maximum amplitude of the H - κ stacking. In this study, we used average crustal P -wave velocities beneath individual stations based on the tomography results of Wu et al. (2009). Zhu and Kanamori (2000) showed that a few percent uncertainties in Vp had negligible effect on the estimated crustal thickness (less than 0.5 km). The weighting factors for Ps, PpPs and PpSs + PsPs were 0.6, 0.3, and 0.1, respectively.

4. Results

4.1. Stacked receiver functions and H - κ stacking analysis

Crustal thickness and Vp/Vs ratio results for all broadband stations are listed in Table 1. The stations were classified into three Grades, A–C, based on the appearance of the receiver functions as defined below. Fig. 3a and b shows results of a Grade-A station TPUB, which has clear Moho Ps and its crustal multiple PpPs in its receiver functions (Fig. 3b). A well-resolved global maximum was located in the H - κ stacking (Fig. 3a). The white ellipse in Fig. 3a shows the $1 - \sigma$ standard deviation. For Grade-A stations, both the crustal thicknesses and Vp/Vs ratios were well resolved. We compared the estimated crustal Vp/Vs ratios with those in the tomography results of Wu et al. (2009). The two agree well for two thirds of the Grade-A stations, with differences within the uncertainty levels (Table 1).

For Grade-B stations, only the Moho Ps can be clearly identified and there were ambiguities to identify its crustal multiples. An

Table 1
 H - κ stacking results of 27 Grade-A and -B broadband stations. The Moho Ps delay times (tps) are measured at ray-parameter of 0.06 s/km.

Station	Lat./Long./Elev., m	No. of RFs	tps, s	H, km	Vp/Vs (κ)	Wu's Vp, km/s	Wu's Vp/Vs	Quality	Bed rock/Geological setting
ALSB	23.51/120.81/2413.4	38	5.0	41.2	–	5.92	1.69	B	Sediment/Western Foothills
ANPB	25.19/121.52/825.7	95	2.8	17.5 ± 3.6	1.90 ± 0.21	5.84	1.71	A	Andesite/Volcanic Area
EASB	22.38/120.85/445.0	41	4.1	32.8	–	5.78	1.70	B	Sediment/Backbone Range
ENLB	23.90/121.60/71.0	27	3.3	22.3	–	5.80	1.84	B	Sediment/Coastal Range
FULB	23.25/121.20/376.0	41	1.7	15.7	–	6.07	1.64	B	Sediment/Eastern Central Range
KMNB	24.46/118.39/43.0	132	3.7	29.5 ± 2.1	1.75 ± 0.10	6.30	–	A	Granite/Continental Crust
LIOB	24.65/121.02/382.0	18	4.2	35.1	–	5.89	1.68	B	Rock/Western Foothills
MATB	26.15/119.95/75.1	86	4.0	32.0 ± 1.6	1.75 ± 0.05	6.30	–	A	Granite/Continental Crust
NACB	24.17/121.59/130.0	134	4.4	37.9 ± 3.1	1.70 ± 0.08	6.25	1.69	A	Marble/Eastern Central Range
NANB	24.52/121.83/112.0	22	5.5	43.5 ± 1.2	1.75 ± 0.03	6.12	1.71	A	Rock/Eastern Central Range
PTSB	24.45/120.71/202.0	7	4.2	30.6	–	5.74	1.76	B	Sediment/Western Foothills
SCZB	22.37/120.63/74.0	35	4.6	36.5	–	5.27	1.64	B	Rock/Backbone Range
SGSB	23.08/120.58/278.0	38	5.3	40.8	–	5.54	1.69	B	Sediment/Western Foothills
SLBB	24.75/121.64/490.0	39	1.9	18.0	–	6.24	1.63	B	Sediment/Hsueshan Range
SSLB	23.79/120.95/450.0	170	6.4	53.5 ± 2.7	1.71 ± 0.06	6.24	1.76	A	Sandstone/Hsueshan Range
TATO	24.98/121.49/53.0	78	3.9	23.6 ± 1.6	1.90 ± 0.07	5.54	1.69	A	Siltstone/Western Foothills
TDCB	24.26/121.26/1280.0	99	4.8	40.6	–	6.15	1.70	B	Slate/Hsueshan Range
TPUB	23.30/120.63/370.0	160	4.6	33.9 ± 1.9	1.81 ± 0.08	6.30	1.71	A	Siltstone/Western Foothills
TWGB	22.82/121.08/195.0	153	1.5	11.4	–	6.42	1.82	B	Meta-Sandstone/Longitudinal Valley
TWHB	22.68/121.48/50.0	17	1.9	12.0 ± 1.6	1.75 ± 0.19	4.91	1.74	A	Andesite/Oceanic Crust
TWKB	21.94/120.81/90.0	148	3.9	31.5 ± 1.5	1.69 ± 0.06	5.75	1.71	A	Sandy Shale/Hengchun Peninsula
TWMB	22.82/120.42/340.0	63	4.5	32.5 ± 1.7	1.74 ± 0.06	5.42	1.80	A	Sediment/Western Foothills
WFSB	25.07/121.78/500.0	81	3.4	19.4 ± 2.2	1.99 ± 0.18	5.74	1.56	A	Siltstone/Western Foothills
WLCB	22.35/120.36/38.0	64	4.9	39.0 ± 1.1	1.60 ± 0.03	4.89	1.82	A	Sediment/Coastal Plain
WLTB	24.86/121.26/27.0	43	3.9	27.5	–	5.35	1.74	B	Sediment/Western Foothills
YHNB	24.67/121.38/775.0	34	3.1	24.9	–	5.69	1.68	B	Slate/Hsueshan Range
YULB	23.39/121.30/294.7	140	1.8	14.6	–	5.71	1.68	B	Black Schist/Eastern Central Range

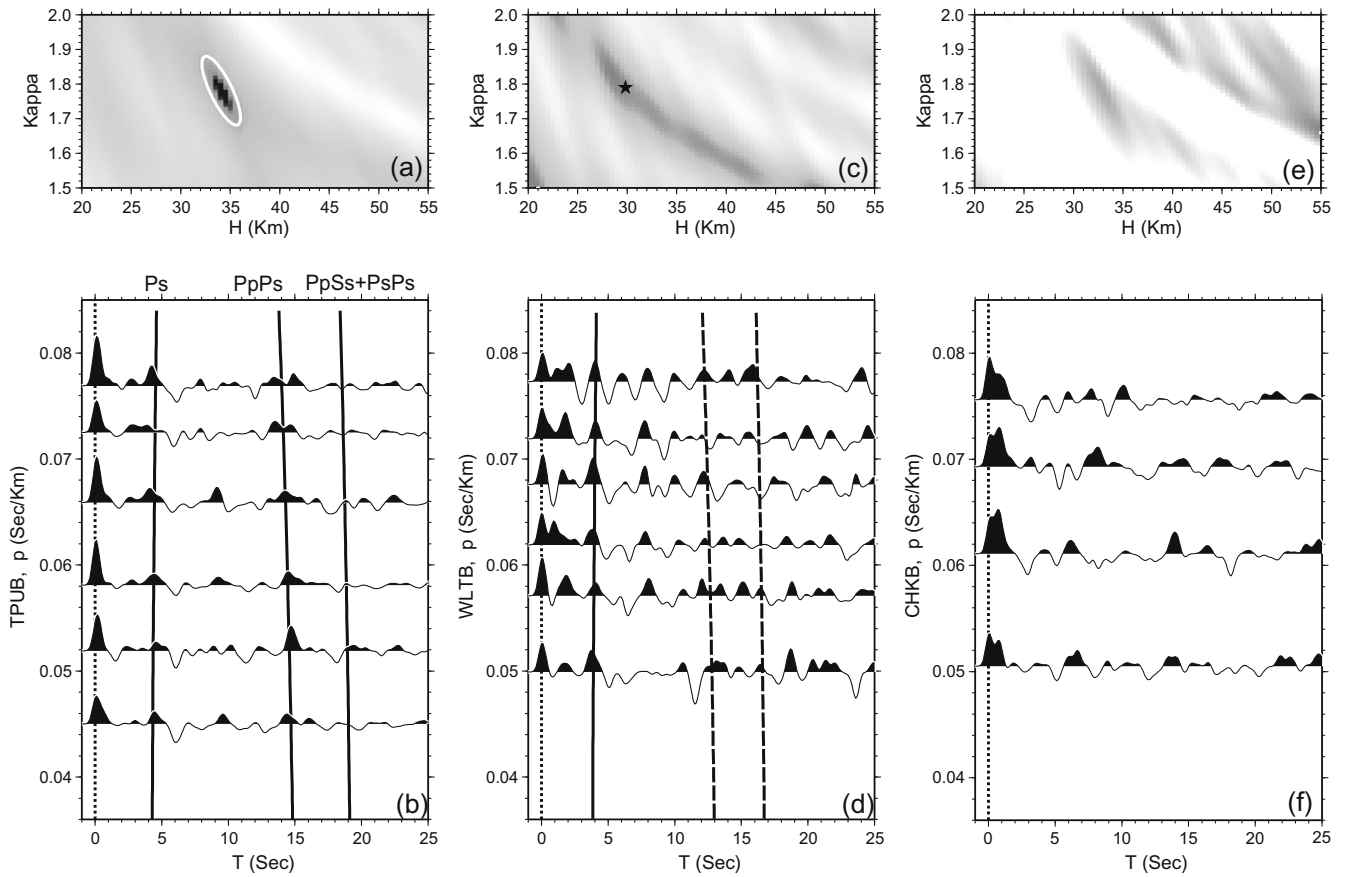


Fig. 3. $H-\kappa$ stacking results of three stations TPUB (a), WLTB (c) and CHKB (e). Their corresponding receiver functions are shown in below. The predicted arrival times of Moho Ps, PpPs and PpSs + PsPs, using the determined crustal thickness and V_p/V_s ratio are indicated.

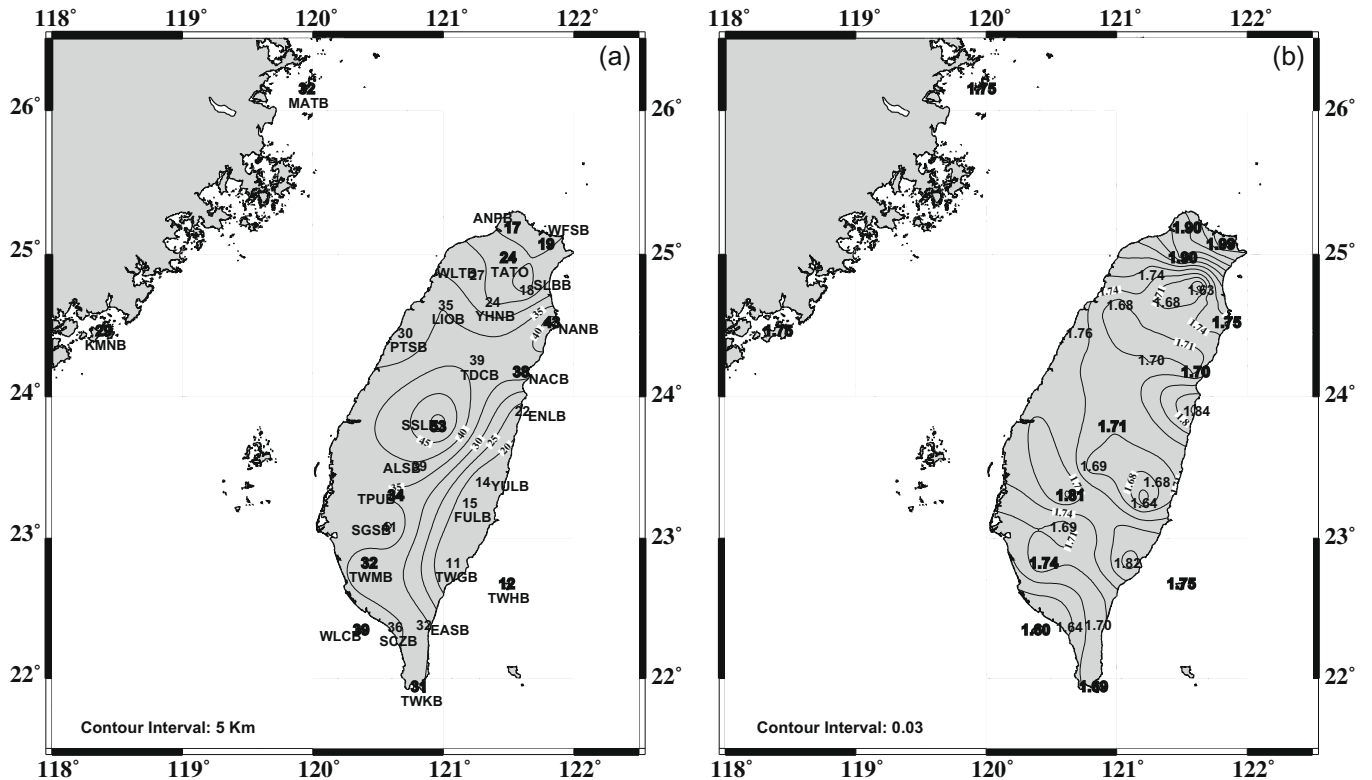


Fig. 4. (a) Moho depth variation and (b) crustal V_p/V_s ratio variation in the Taiwan region. The contours of the Moho depth and the κ values are only determined from the results of 27 Grade-A (boldface numbers) and -B stations (regular numbers).

example is shown in Fig. 3c and d using station WLTB. The two dashed lines represent possible locations of the PpPs and PpSs+PsPs phases. No well-defined global maximum could be found from the $H-\kappa$ stacking and a strong trade-off exists between the crustal thickness and V_p/V_s ratio (Fig. 3c). For Grade-B stations, we used the averaged crustal V_p/V_s ratio in the tomographic results of Wu et al. (2009) beneath the station to determine the crustal thickness.

For Grade-C stations, none of the Moho converted phases could be identified. Fig. 3e and f shows an example of station CHKB. Most Grade-C stations are located in sedimentary basins where the strong P-to-S converted waves at the bottom of the basin mask out the later Moho converted phases. Receiver functions at one off-shore station, LYUB, also show complicated waveforms that may be due to the complex sea-land interface. No crustal thickness and V_p/V_s ratio were obtained from Grade-C stations.

4.2. Crustal structures of Taiwan

Fig. 4a and b shows the Moho depth variation and the κ value distribution beneath the whole Taiwan area estimated by the $H-\kappa$ stacking analysis method. In general, the Moho is shallow in northern and southeastern Taiwan and becomes deep in the central and southwestern parts of Taiwan.

Relatively simple receiver functions and well-resolved crustal thicknesses and V_p/V_s ratios beneath stations KMNB and MATB reflect a typical stable continental crust of about 30 km thick. Stations ANPB and WFSB in northern Taiwan reveal a shallow Moho at about 17–19 km in depth and a relative high V_p/V_s ratio of about

1.90, which is probably associated with the Tatun and Keelung volcanic activities. The thin crust (11–15 km) east of the Longitude Valley suture belongs to the oceanic lithosphere of the Philippine Sea plate. The abnormal deep Moho of 43 km beneath NANB in northern Taiwan is likely caused by the collision of the Ryukyu Arc and subduction of Philippine Sea slab (Font et al., 2001). The deepest Moho was found to be 53 km beneath station SSLB in central Taiwan. The Moho beneath station ALSB near SSLB is also relatively deep (39 km). The Moho depth in southern Taiwan varies from 31 km down to 39 km. In addition, the V_p/V_s ratio varies from 1.60 to 1.74 and is lower than the global average of 1.78 for Mesozoic–Cenozoic orogenic belts (Zandt and Ammon, 1995). The low V_p/V_s ratios probably represent a felsic crustal bulk composition (e.g. Christensen, 1996; Zandt and Ammon, 1995).

5. Discussion and conclusions

The Bouguer gravity anomaly often reflects subsurface density and crustal thickness variation. Assuming a relatively constant crustal density, large positive Bouguer gravity anomalies correspond to thin crust and negative Bouguer gravity anomalies correspond to thick crust. Fig. 5a shows a comparison between Bouguer gravity anomaly map in Taiwan by Yen and Yeh (1998) and our Moho depth variation. In general, the two agree with each other. The largest negative Bouguer anomaly is located in central Taiwan where the crust is thickest. In Fig. 5b we plotted Bouguer gravity anomalies vs. Moho depths at 25 stations located in the Taiwan island. The gray-colored line represents the expected gravity

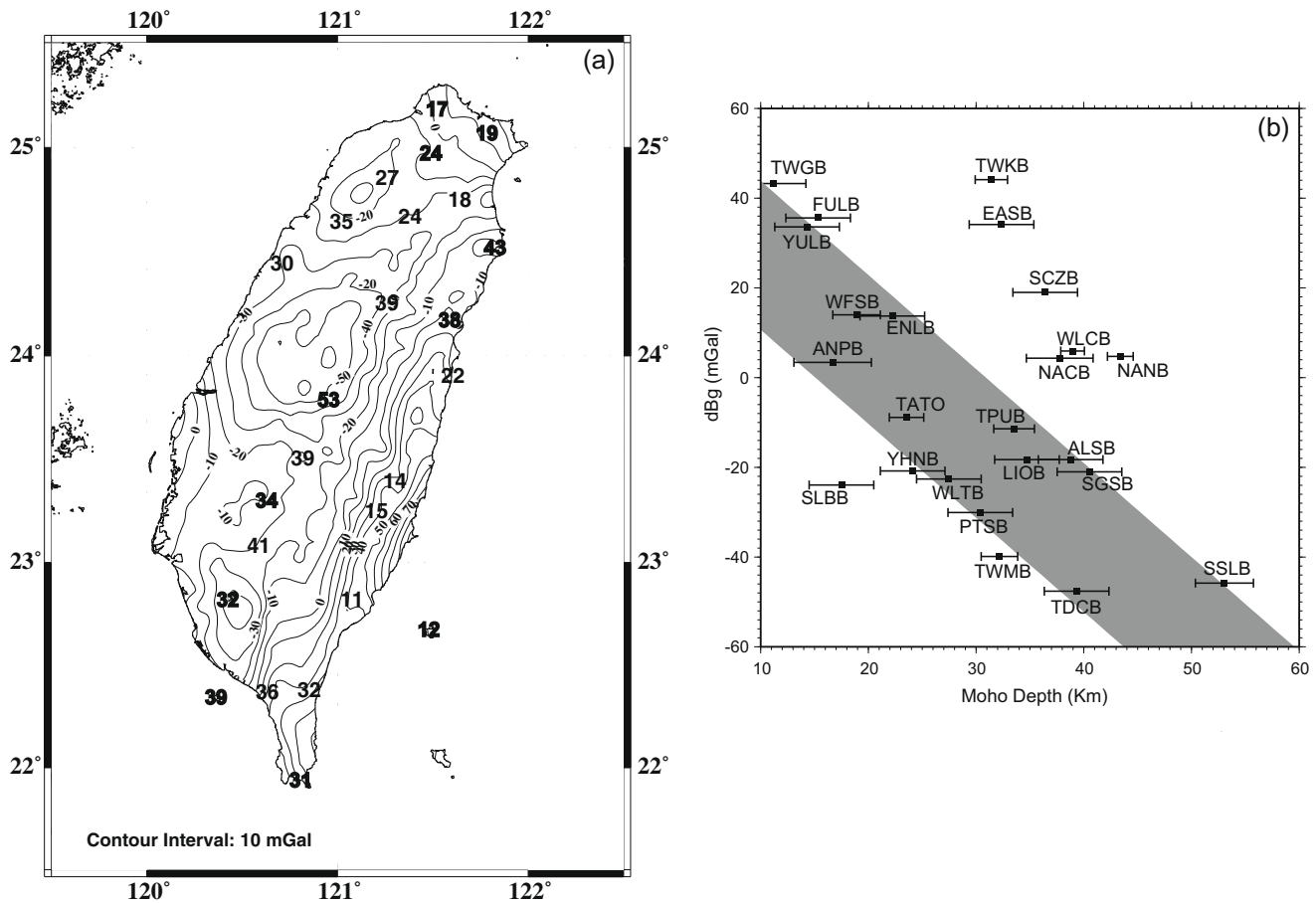


Fig. 5. (a) Comparison between the Moho depth variation in Fig. 4 and Bouguer gravity anomaly of Yen and Yeh (1998). The boldface numbers are for Grade-A stations and regular numbers are for Grade-B stations. (b) Comparison of Moho depths and Bouguer gravity anomalies at 25 stations in the Taiwan Island. The gray-colored line represents the predicted gravity anomalies produced by Moho undulation with a constant density contrast of 500 kg/m³.

anomalies caused by Moho undulation with a constant density contrast of 500 kg/m³. We did not correct the gravity anomalies for sedimentary thickness variation, which maybe significant for stations WLTB, PTSB, LIOB and TWMB located in western Taiwan. Nevertheless, Fig. 5b shows that a large portion of the observed Bouguer gravity anomalies in Taiwan can be explained by crustal thickness variation. It can also be seen that stations NANB, NACB, EASB, TWKB, SCZB, and WLCB have large positive gravity anomalies, after taking into account the Moho depth undulation. They are located near the places where the Philippine Sea Plate subducts beneath Ryukyu Arc and the Eurasian plate subducts beneath the Luzon Arc (Fig. 1). The large positive gravity anomalies are therefore likely a manifestation of the high-density slab in the mantle beneath.

Overall, the crustal thickness variation results indicate that the collision between the Philippine Sea plate and Eurasian plate in Taiwan involves the whole crust, not just the upper crust as suggested by the thin-skinned tectonics model. In front of the thin Philippine sea crust, the crust in Central Taiwan has been thickened to more than 50 km, nearly doubling its original thickness as represented by the crust thicknesses beneath stations KMNB and MATB to the west. In northeastern Taiwan (stations NANB and NACB) and southwestern Taiwan (station WLCB) where the island connects to the Ryukyu Arc and Luzon Arc, the crust has also been substantially thickened.

In summary, we present an updated crustal thickness model of Taiwan based on all available permanent seismic stations and the teleseismic receiver function method. The results show very thin crust (11–15 km) east of the Longitude Valley suture zone. Moho is shallow in northern and southeastern part of Taiwan (17–32 km), becomes deep in southwestern (32–39 km), and reaches the deepest depth in central Taiwan (53 km). The relatively shallow Moho (~20 km) and high Vp/Vs ratio (~1.90) in northern Taiwan are probably associated with the Tatun and Keelung volcanism. The thick crust and the corresponding large negative Bouguer gravity anomaly in western-central Taiwan suggest crustal thickening by the collision between the Philippine Sea plate and Eurasian plate.

Acknowledgments

We are grateful to Dr. Wen-Tzong Liang of IES, Dr. Rong-Yuh Chen and Mr. Chih-Wen Kan of CWB for their help to download seismic waveform data. Special thanks to Prof. Hung-Yuan Yen who provided the Bouguer gravity data and to Prof. Yih-Min Wu for providing seismic tomography results. The authors would also like to thank Drs. Jer-Ming Chiu, Francis T. Wu, Wang-Ping Chen and Honn Kao for the encouragements and constructive discussions. Constructive comments from Dr. Jordi Julia and one anonymous reviewers greatly help to improve the manuscript. This study was supported by the National Science Council (NSC92-2119-M-194-008) with TEC contribution.

References

Ammon, C.J., 1991. The isolation of receiver effects from teleseismic *P* waveforms. *Bulletin of the Seismological Society of America* 81, 2504–2510.

- Christensen, N.L., 1996. Poisson's ratio and crustal seismology. *Journal of Geophysical Research* 101, 3139–3156.
- Font, Y., Liu, C.S., Schnurle, P., Lallemand, S., 2001. Constraints on backup geometry of the southwest Ryukyu subduction based on reflection seismic data. *Tectonophysics* 333, 135–158.
- Hsu, S.-K., Sibuet, J.-C., 1995. Is Taiwan the result of arc-continent or arc-arc collision? *Earth and Planetary Science Letters* 136, 315–324.
- Kim, K.-H., Chiu, J.-M., Kao, H., Liu, Q., Yeh, Y.-H., 2004. A preliminary study of crustal structure in Taiwan region using receiver function analysis. *Geophysical Journal International* 159, 146–164.
- Kim, K.H., Chiu, J.M., Pujol, J., Chen, K.C., Huang, B.S., Yeh, Y.H., Shen, P., 2005. Three-dimensional Vp and Vs structural model associated with the active subduction and collision tectonics in the Taiwan region. *Geophysical Journal International* 162, 204–220.
- Langston, C.A., 1979. Structure under Mount Rainier, Washington, inferred from teleseismic body waves. *Journal of Geophysical Research* 84, 4749–4762.
- Ligorria, J.P., Ammon, C.J., 1999. Iterative deconvolution and receiver-function estimation. *Bulletin of the Seismological Society of America* 89, 1395–1400.
- Lin, A.T., Watts, A.B., 2002. Origin of the West Taiwan Basin by orogenic loading and flexure of a rifted continental margin. *Journal of Geophysical Research*, 107. doi:10.1029/2001JB000669.
- Lin, A.T., Watts, A.B., Hesselbo, S.P., 2003. Cenozoic stratigraphy and subsidence history of the South China Sea margin in the Taiwan region. *Basin Research* 15, 453–478.
- Ma, K.F., Wang, J.H., Zhao, D., 1996. Three-dimensional seismic velocity structure of the crust and uppermost mantle beneath Taiwan. *Journal of Physical Earth* 44, 85–105.
- Phinney, R.A., 1964. Structure of earth's crust from spectral behavior of long-period body waves. *Journal of Geophysical Research* 69, 2997–3017.
- Rau, R.-J., Wu, F.T., 1995. Tomographic imaging of lithospheric structures under Taiwan. *Earth and Planetary Science Letters* 133, 517–532.
- Roecker, S.W., Yeh, Y.H., Tsai, Y.B., 1987. Three-dimensional P and S wave velocity structures beneath Taiwan: deep structure beneath an arc-continent collision. *Journal of Geophysical Research* 92, 10547–10570.
- Shin, T.C., Chen, Y.L., 1988. Study on the earthquake location of 3-D velocity structure in the Taiwan area. *Meteorological Bulletin* 42, 135–169.
- Sibuet, J.C., Hsu, S.K., 2004. How was Taiwan created? *Tectonophysics* 379, 159–181.
- Suppe, J., 1981. Mechanics of mountain-building and metamorphism in Taiwan. *Memoir of the Geological Society of China* 4, 67–90.
- Teng, L.S., Lin, A.T., 2004. Cenozoic Tectonics of the Southeast China continental margin: insight from Taiwan. In: Malpas, J., Fletcher, C.J., Aitchinson, J.C., Ali, J. (Eds.), *Aspects of the Tectonic Evolution of China*, Special Publications ed., 226. Geological Society, London, pp. 313–332.
- Tomfohrde, D.A., Nowack, R.L., 2000. Crustal structure beneath Taiwan using frequency-band inversion of receiver function waveforms. *Pure and Applied Geophysics* 157, 737–764.
- Wang, H.-L., Chen, H.-W., Zhu, L., submitted for publication. Constraints on average Moho geometry beneath Taiwan—Receiver function analysis using BATS Data. *Geophysical Journal International*.
- Wu, F.T., Rau, R.-J., Salzberg, D., 1997. Taiwan orogeny: think-skinned or lithospheric collision? *Tectonophysics* 274, 191–220.
- Wu, Y.-M., Chang, C.-H., Zhao, L., Shyu, J.B.H., Chen, Y.-G., Sieh, K., Avouac, J.-P., 2007. Seismic tomography of Taiwan: Improved constraints from a dense network of strong motion stations. *Journal of Geophysical Research*, 112. doi:10.1029/2007JB004983.
- Wu, Y.-M., Shyu, J.B.H., Chang, C.-H., Zhao, L., Nakamura, M., Hsu, S.K., 2009. Improved seismic tomography offshore northeastern Taiwan: Implications for subduction and collision processes between Taiwan and the southernmost Ryukyu. *Geophysical Journal International* 178, 1042–1054.
- Yeh, H.Y., Yeh, Y.H., 1998. Two-dimensional crustal structures of Taiwan from gravity data. *Tectonics* 17, 104–111.
- Yu, S., Chen, H.Y., Kuo, L.C., 1997. Velocity field of GPS stations in the Taiwan area. *Tectonophysics* 274, 41–59.
- Zandt, G., Ammon, C.J., 1995. Continental crust composition constrained by measurements of crustal Poisson's ratio. *Nature* 374, 152–154.
- Zhu, L., Kanamori, H., 2000. Moho depth variation in southern California from teleseismic receiver functions. *Journal of Geophysical Research* 105, 2969–2980.
- Zhu, L., Zeng, R.S., Wu, F.T., Owens, T.J., Randall, G.E., 1993. Preliminary study of crust-upper mantle structure of the Tibetan plateau by using broadband teleseismic body waveforms. *Acta Seismologica Sinica* 6, 305–316.